Fast Multipole Acceleration of the Hybrid Finite Element-Boundary Element Analysis of 3D Eddy Current Problems

R. V. Sabariego, J. Gyselinck, P. Dular, C. Geuzaine and W. Legros

***Abstract*— This paper deals with the acceleration of the hybrid finite element – boundary element analysis of 3D eddy current problems by means of the fast multipole method. An adaptive truncation scheme for the multipole expansion of the 3D Laplace Green function is proposed. As an application example, the TEAM workshop problem 28 is considered. The computational cost without and with fast multipole acceleration is discussed.**

***Index Terms*— fast multipole method, hybrid techniques, finite element method, boundary element method, Laplace function**

I. Introduction

HYBRID finite element – boundary element (FE-BE) models are particularly suited for solving open electromagnetic field problems that comprise movement, nonlinear media and eddy currents [1]. The finite element (FE) method easily accounts for saturable and conducting media, while the boundary element (BE) method provides a rigorous treatment for open problems and allows to consider movement without any tedious mesh manipulations (remeshing or moving band definition). However, the BE part of the hybrid model generates dense blocks in the system matrix and significantly limits the problem size.

The fast multipole method (FMM) [2], combined with an iterative solver, e.g. GMRES [3], can be employed to overcome this limitation by diminishing both the storage requirements and the computation time. It has been successfully applied to BE models in both the high frequency [4] and the low frequency domain [5], [6]. Its use with hybrid FE-BE models has been mainly tackled in scattering applications [7].

This paper deals with the application of the FMM to the hybrid FE-BE analysis of 3D low frequency eddy current problems. Section II outlines the hybrid modelling of a magnetodynamic problem. The FMM is briefly described in the following section. An adaptive truncation scheme for the 3D Laplace Green function is used. Some aspects relative to the application of the FMM to a problem with moving parts are briefly discussed.

As test case, the TEAM workshop problem 28 is considered [8]. The transient behaviour is modelled taking into account the eddy currents and the mechanical equation.

II. 3D Hybrid FE-BE model

We consider a magnetodynamic problem in $\mathbb{R}^3$. The FE method is used in a domain Ω with boundary Γ while the BE method takes into account the space exterior to Ω. The eddy current conducting part of Ω is denoted Ω_c and the non-conducting one Ω_c^C. Source conductors, with a given current density $\underline{j}_s$, are comprised in $\Omega_s \subset \Omega_c^C$.

Adopting the magnetic field formulation, the general expression of the magnetic field $\underline{h}$ in Ω is

$$\underline{h} = \underline{h}_s + \underline{h}_r - \mathrm{grad}\phi, \tag{1}$$

with $\underline{h}_s$ a source field satisfying $\mathrm{curl}\,\underline{h}_s = \underline{j}_s$, $\underline{h}_r$ the reaction field in Ω_c, and ϕ the reaction magnetic scalar potential in Ω_c^C. The source magnetic field $\underline{h}_s$ obeying $\mathrm{curl}\,\underline{h}_s = \underline{j}_s$ is not unique. The one calculated by the Biot-Savart law implicitely satisfies $\mathrm{div}\,\underline{h}_s = 0$.

The $\underline{h} - \phi$ magnetodynamic formulation is obtained from the weak form of the Faraday law:

$$\partial_t(\mu\underline{h}, \underline{h}')_\Omega + (\sigma^{-1}\mathrm{curl}\,\underline{h}, \mathrm{curl}\,\underline{h}')_{\Omega_c} + (\sigma^{-1}\underline{j}_s, \mathrm{curl}\,\underline{h}')_{\Omega_s} + \partial_t\langle \underline{n}\cdot\underline{b}, \phi'\rangle_\Gamma = 0, \quad \forall\, \underline{h}' \in F_{h\phi}(\Omega), \tag{2}$$

where μ is the magnetic permeability, σ is the electric conductivity; $\underline{n}$ is the unit normal vector on Γ pointing into Ω; $(\cdot,\cdot)_\Omega$ and $\langle\cdot,\cdot\rangle_\Gamma$ denote a volume integral in Ω and a surface integral on Γ of the product of their arguments; $F_{h\phi}(\Omega)$ is the function space defined on Ω and containing the basis functions for $\underline{h}$ (coupled to ϕ) as well as for the test function $\underline{h}'$ [10].

The coupling with the BE model is done through the surface integral in (2). We define the following integral operator:

$$\mathcal{P}(q) = \int_\Gamma q\, G\, \mathrm{d}\Gamma \quad \text{with} \quad G(\rho) = \frac{1}{4\pi\rho}, \tag{3}$$

where q is an equivalent magnetic charge on Γ and $G(\rho)$ is the 3D Laplace Green function, ρ being the distance between a source point $\underline{r}_s$ (on Γ) and an observation point $\underline{r}_o$ (in $\mathbb{R}^3\backslash\Omega$). The normal derivative of (3a) in a point on Γ is given by

$$\underline{n}\cdot\mathrm{grad}\,\mathcal{P}(q) = \frac{1}{2}q + \int_\Gamma q\,\underline{n}\cdot\mathrm{grad}\,G\ \mathrm{d}\Gamma. \tag{4}$$

The scalar potential and its normal derivative in a point on Γ can be expressed as

$$\phi(\underline{r}) = \mu^{-1}\,\mathcal{P}(q)\,, \quad \underline{n}\cdot\mathrm{grad}\,\phi(\underline{r}) = \mu^{-1}\underline{n}\cdot\mathrm{grad}\,\mathcal{P}(q)\,. \tag{5}$$

The surface term in (2) thus becomes

$$\partial_t\langle\underline{n}\cdot\underline{b}, \phi'\rangle_\Gamma = -\partial_t\langle\underline{n}\cdot\mathrm{grad}\,\mathcal{P}(q), \phi'\rangle_\Gamma + \partial_t\langle\mu\underline{n}\cdot\underline{h}_s, \phi'\rangle_\Gamma\,. \tag{6}$$

The weak form of (5a) reads:

$$\langle\phi, q'\rangle_\Gamma = \langle\mu^{-1}\mathcal{P}(q), q'\rangle_\Gamma, \quad \forall q' \in F_q(\Gamma)\,, \tag{7}$$

Manuscript received July 3, 2003. The research has been carried out in the frame of the Inter-University Attraction Poles IAP P5/34 funded by the Belgian federal goverment.

The authors are with the Department of Electrical Engineering, Institut Montefi ore, University of Liège, Sart Tilman Campus, Building B28, B-4000 Liège, Belgium (email: r.sabariego@ulg.ac.be). P. Dular and C. Geuzaine are Research Associate and Postdoctoral Researcher with the Belgian National Fund for Scientifi c Research (F.N.R.S.).

where $F_q(\Gamma)$ is the function space defined on Γ which contains the basis functions for q and the test function q'.

Applying the Galerkin method to the equations (2) and (7), the system of equations of the hybrid model is obtained. Edge basis functions are employed for $\underline{h}$, resulting in sparse blocks in the matrix system. The terms with the integral operator $\mathcal{P}(q)$ (3) give dense blocks. Let us consider, e.g. the fully populated block $\boldsymbol{M}$ due to the right handside of (7).

On the basis of the discretisation of Γ, n_q interpolation functions $\beta_l(\underline{r})$ are defined for the equivalent magnetic charge q and their coefficients q_l are assembled in the column matrix $\boldsymbol{Q}$:

$$q(\underline{r}) = \sum_{l=1}^{n_q} q_l\, \beta_l(\underline{r}) \quad \text{and} \quad \boldsymbol{Q} = \left[\ q_1\ \ldots\ q_{n_q}\ \right]^T . \tag{8}$$

The elements of $\boldsymbol{M}$ are then given by

$$M_{k,l} = \frac{1}{\mu} \oint_\Gamma \beta_k \left(\oint_\Gamma \beta_l\, G \,\mathrm{d}\Gamma \right) \mathrm{d}\Gamma \,. \tag{9}$$

The double integration is a critical and time-consuming stage for the assembly of the BE blocks, especially when numerical integration is used. The number of Gauss integration points required for accurately evaluating the self-interactions is high. If plane triangular elements and piecewise constant or linear basis functions are used for $q(\underline{r})$, the inner integral in (9) can be evaluated analytically [9]. The outer integration can be performed adaptively with numerical Gauss integration.

III. Fast Multipole Method

The fast multipole method (FMM) decomposes the boundary Γ into $\#g$ groups of elements, $\Gamma = \bigcup_{g=1}^{\#g} \Gamma_g$, and determines the interactions between distant groups by means of the multipole expansion of the Green function. The simplest way to

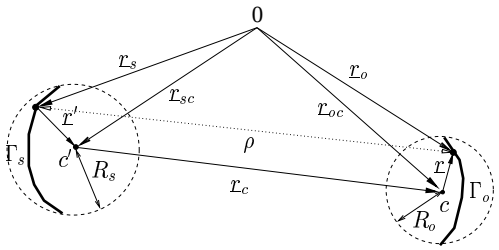

Fig. 1. Distant groups Γ_s and Γ_o on the contour Γ with centers c' and c

distribute the elements in groups consists in building an octree [5], [6]. Note that in a single level FMM, as described in the present paper, only the finest level of the octree is taken into account.

A. Multipole expansion of the 3D Laplace Green function

Let Γ_s be a source group with center $\underline{r}_{sc}$ and a source point $\underline{r}_s$, and Γ_o an observation group with center $\underline{r}_{oc}$ and an observation point $\underline{r}_o$. We define the vectors $\underline{r} = \underline{r}_o - \underline{r}_{oc} = (r, \theta, \phi)$, $\underline{r}_c = \underline{r}_{oc} - \underline{r}_{sc} = (r_c, \theta_c, \phi_c)$ and $\underline{r}' = \underline{r}_{sc} - \underline{r}_s = (r', \theta', \phi')$ as shown in Fig. 1. Omitting the factor $1/4\pi$, the 3D Laplace Green function (3b), with $\rho = |\underline{r}_o - \underline{r}_s|$, is expanded as [2]:

$$\frac{1}{\rho} = \Re\Big(\sum_{m=0}^{\infty} \sum_{n=-m}^{m} \sum_{u=0}^{\infty} \sum_{v=-u}^{u} \mathcal{D}_{m,n}\, \mathcal{T}_{m+u,n+v}\, \mathcal{A}_{u,v} \Big) , \tag{10}$$

$$\mathcal{D}_{m,n}\,(\underline{r}) = \frac{r^m\, \mathcal{L}_n^m(\theta, -\phi)}{(m+n)!} , \tag{11}$$

$$\mathcal{T}_{m+u,n+v}\,(\underline{r}_c) = \frac{(m+u-(n+v))!}{r_c^{m+u+1}}\, \mathcal{L}_{m+u}^{n+v}(\theta_c, \phi_c) , \tag{12}$$

$$\mathcal{A}_{u,v}\,(\underline{r}') = \frac{r'^u\, \mathcal{L}_u^v(\theta', -\phi')}{(u+v)!} , \tag{13}$$

where $\mathcal{L}_n^m(\theta, \phi) = P_m^n(\cos\theta)\, e^{\imath n \phi}$, P_m^n being the Legendre function of degree m and order n. The imaginary number is denoted $\imath$ and $\Re$ indicates the real part.

In practice, the multipole expansion (10) must be truncated by taking $0 \le m \le p$ and $0 \le u \le p$, where the truncation number p must be sufficiently large to limit the error to a prescribed value ε. In most cases, the conventional choice $p = \log_2(1/\varepsilon)$ [2] is too conservative. Indeed, if $r' \ll r_c$ and $r \ll r_c$, a smaller number of terms suffices. A more economic law, proposed by the authors for the 2D case in [11], takes those distances into account. Let us consider the radii of the source and observation groups, $R_s = \max_{\Gamma_s}(r')$, $R_o = \max_{\Gamma_o}(r)$, and the distance between their centers $d = r_c$. The minimum value of p as a function of R_o/d and R_s/d for $\varepsilon = 10^{-6}$ is depicted in Fig. 2.

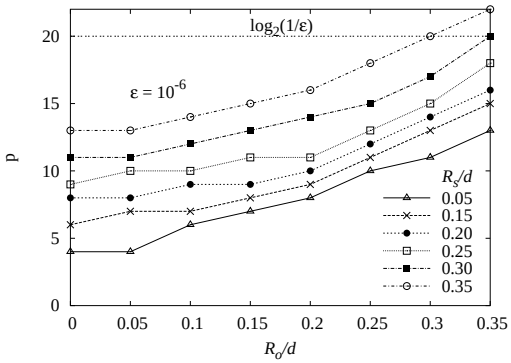

Fig. 2. Truncation number $p(R_o/d, R_s/d)$ for $\varepsilon = 10^{-6}$

The function $\mathrm{grad}\, G$ can be expanded in a similar way. It suffices to derive (11) with respect to the coordinates of the observation point.

B. Application to the BE part of the hybrid FE-BE model

Two groups Γ_s and Γ_o are said to be 'far' groups if $R_s/d < \tau$ and $R_o/d < \tau$, where d is the distance between the group centers and where τ is chosen smaller than 1/2.

The dense blocks due to the BE part and in particular $\boldsymbol{M}$ (9) can be formally written as

$$\boldsymbol{M} \;\approx\; \boldsymbol{M}^{near} + \boldsymbol{M}^{far} \;=\; \boldsymbol{M}^{near} + \underbrace{\sum_{o=1}^{\#g} \sum_{s=1}^{\#g}}_{\Gamma_o,\, \Gamma_s \text{ far}} \boldsymbol{M}_{o,s}^{far} . \tag{14}$$

Let us consider the degrees of freedom q_k and q_l of q with associated basis functions $\beta_k(\underline{r}_o)$ and $\beta_l(\underline{r}_s)$ that are nonzero on the respective far groups Γ_o and Γ_s. Substituting (10) in (9), the contribution to the corresponding element $\left(\boldsymbol{M}_{o,s}^{far}\right)_{k,l}$ in $\boldsymbol{M}^{far}$ is given by

$$\Re\left(\sum_{m=0}^{p} \sum_{n=-m}^{m} \boldsymbol{M}_{o,k,m,n}^{\mathcal{D}} \sum_{u=0}^{p} \sum_{v=-u}^{u} \boldsymbol{M}_{m+u,n+v}^{\mathcal{T}} \boldsymbol{M}_{s,l,u,v}^{\mathcal{A}} \right), \tag{15}$$

$$\boldsymbol{M}^{\mathcal{D}}_{o,k,m,n} = \int_{\Gamma_o} \beta_k \mathcal{D}_{m,n}\,\mathrm{d}\Gamma\,, \quad \boldsymbol{M}^{\mathcal{A}}_{s,l,u,v} = \int_{\Gamma_s} \beta_l \mathcal{A}_{u,v}\,\mathrm{d}\Gamma\,, \quad (16)$$

$$\boldsymbol{M}^{\mathcal{T}}_{m+u,n+v} = \frac{1}{4\pi\mu}\mathcal{T}_{m+u,n+v}\,. \quad (17)$$

The aim of the formal decomposition (15) is speeding up the multiplication of $\boldsymbol{M}^{far}$ by a trial vector $\boldsymbol{Q}$, required for the iterative solution of the system of algebraic equations. Group by group, the field produced by the equivalent magnetic charge q in the considered group is aggregated into its center by (16b). This aggregated field is then subsequently translated to the centers of all the far groups by (17), and finally the aggregated and translated field is disaggregated into the degrees of freedom of the far groups thanks to (16a).

The multiplication $\boldsymbol{M}^{far}\boldsymbol{Q}$ is further accelerated by means of the adaptive truncation scheme following the law $p = p(R_s/d, R_o/d, \varepsilon)$ shown in Fig. 2. In case of preconditioning of the iterative solver, the preconditioner is based on the sparse matrix comprising the complete FE contribution but only the BE near-field interactions.

The assembly stage of the FMM consists in calculating and storing the required complex numbers $\boldsymbol{M}^{\mathcal{D}}_{o,k,m,n}$, $\boldsymbol{M}^{\mathcal{T}}_{m+u,n+v}$ and $\boldsymbol{M}^{\mathcal{A}}_{s,l,u,v}$. The matrix $\boldsymbol{M}^{far}$ itself is never built. The integrations in (16) are done numerically but as we are dealing with far interactions a limited number of Gauss integration point suffices. The matrix $\boldsymbol{M}^{near}$ is calculated in the conventional way (see previous section) and stored using a sparse storage scheme. For the $\boldsymbol{M}^{\mathcal{D}}$ and $\boldsymbol{M}^{\mathcal{A}}$ data of a given group, the truncation number p considered during the FMM assembly stage is determined by its closest far group, $p = p_{max}$. For the $\boldsymbol{M}^{\mathcal{T}}$ data, the truncation number p is determined by the two groups Γ_s and Γ_o involved in the translation, $p = p_{so}$. During the iterative process, the aggregation step is carried out with $p = p_{max}$, while $p = p_{so}$ suffices for the translation and disaggregation.

As a rule of thumb, the optimum value of τ lies in the interval $[1/4, 1/5]$, i.e., an observation group Γ_o is far from a source group Γ_s if it is outside the sphere of radius $R_{far} \in [3R_s, 4R_s]$ with origin the center of Γ_s. The upper limit corresponds to $\tau \leq 1/5$, or, according to Fig. 2, to a maximum truncation number $p_{max} = 10$ for $\varepsilon = 10^{-6}$, while the classical law leads to $p = \log_2(1/\varepsilon) = 20$.

C. Taking movement into account

The analysis is restricted to rigid bodies, the boundaries of which constitute the BE domain. The decomposition in groups $\Gamma = \bigcup_{g=1}^{\#g} \Gamma_g$ is preserved during movement. We define the vectors $\underline{r}^p = \underline{r}^p_o - \underline{r}^p_{oc} = (r, \theta^p, \phi^p)$, $\underline{r}^p_c = \underline{r}^p_{oc} - \underline{r}^p_{sc} = (r^p_c, \theta^p_c, \phi^p_c)$ and $\underline{r}'^p = \underline{r}^p_{sc} - \underline{r}^p_s = (r', \theta'^p, \phi'^p)$ for the new position analogously to the ones shown in Fig. 1.

It is easy to find the relations between the previous and the new FMM data. Indeed, from (16-17), it follows:

$$\boldsymbol{M}'^{\mathcal{D}}_{o,k,m,n} = \boldsymbol{M}^{\mathcal{D}}_{o,k,m,n}\,\frac{\mathcal{L}^m_n(\theta^p, -\phi^p)}{\mathcal{L}^m_n(\theta, -\phi)}\,, \quad (18)$$

$$\boldsymbol{M}'^{\mathcal{T}}_{m+u,n+v} = \boldsymbol{M}^{\mathcal{T}}_{m+u,n+v}\left(\frac{r^p_c}{r_c}\right)^{m+u+1}\frac{\mathcal{L}^{n+v}_{m+u}(\theta^p_c, \phi^p_c)}{\mathcal{L}^{n+v}_{m+u}(\theta_c, \phi_c)}\,, \quad (19)$$

$$\boldsymbol{M}'^{\mathcal{A}}_{s,l,u,v} = \boldsymbol{M}^{\mathcal{A}}_{s,l,u,v}\,\frac{\mathcal{L}^v_u(\theta'^p, -\phi'^p)}{\mathcal{L}^v_u(\theta', -\phi')}\,. \quad (20)$$

This way, the integrals (16-17) do not have to be reevaluated. For updating the disaggregation, aggregation and translation data, a multiplication of the previous data with the corresponding factor suffices. In the particular case of purely translational movement, only the translation data have to be modified.

IV. Application Example

The electrodynamic levitation device of TEAM workshop problem 28 [8] is chosen as test case.

A. Description of the problem

It concerns a cylindrical aluminium plate ($\sigma = 3.40\,10^7$ S/m, radius = 65 mm, thickness = 3 mm, mass = 0.107 kg) located above two coaxial coils carrying imposed sinusoidal currents of amplitude 20 A and frequency 50 Hz (see Fig. 3). The levitation height z refers to the distance between the lower circular end of the cylindrical plate and the upper sides of the coils ($z = 0$).

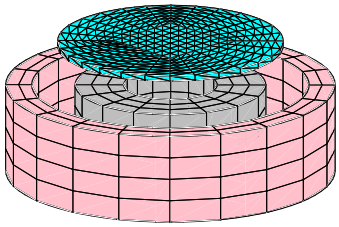

Fig. 3. Levitation device model: cylindrical plate above two coaxial coils

At $t = 0$ the plate rests above the coils at a distance of $z = 3.8$ mm. For $t \geq 0$, sinusoidal currents flow in the coils in opposite directions.

The coils generate a time-varying magnetic field that induces eddy currents in the conducting plate Ω_c and a repulsive vertical force $\underline{F}_{mag}$ is exerted on it. After some damped oscillations the plate reaches a stationary levitation height of $z = 11.3$ mm (measured). The movement is purely translational due to the symmetry of the problem.

The source magnetic field $\underline{h}_s$ is calculated by means of the Biot-Savart law. To this end, the inner and outer coils are discretised in 192 and 160 hexaedra respectively (see Fig.3). The FE domain Ω can be thus restricted to the conducting plate Ω_c. We adopt edge basis fuctions for $\underline{h}$ and piecewise linear basis functions for q.

Different levels of mesh refinement are considered. When the FMM is applied, the surface Γ is split up into 36, 45, 60 or 77 groups depending on the discretisation (see Fig. 4). The optimal number of FMM groups increases with the number of unknowns.

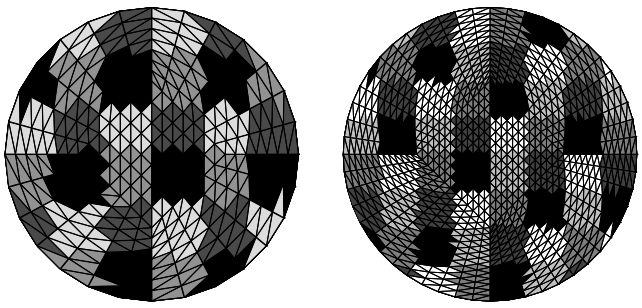

Fig. 4. Distribution in 36 (right) and 60 (left) groups of the plate

For the problem at hand, the FMM integrals (16-17) are evaluated only once. As there is only one BE surface Γ and the

movement is purely translational, they are independent of the position of the plate.

The system of algebraic and differential equations (2) and (7) is time-stepped along with the mechanical equation using the backward Euler scheme. A time interval of $[0, 600\ \mathrm{ms}]$ is studied with $\Delta t = 0.2$ ms (3000 time steps) and $\Delta t = 0.4$ ms (1500 time steps). We adopt the so-called weak electromechanical coupling, i.e. the electromagnetic system and the mechanical equation are solved alternately obtaining and the new magnetic force and the new position, respectively.

The magnetic force $\underline{F}_{mag}$ exerted on conductors Ω_c can be calculated by means of Lorentz law:

$$\underline{F}_{mag} = \int_{\Omega_c} \underline{j} \times \underline{b}\ \mathrm{d}\Omega_c\,. \tag{21}$$

B. Calculation results

The transient behaviour of the levitation device is simulated using a hybrid FE-BE discretisation consisiting of 1280 tetrahedra and 1344 triangles, which yields 1993 unknowns: 1473 for $\underline{h}$ and 520 for q. This is the coarsest mesh in Table I. The optimal group distribution (for this particular mesh) is found to be 36 groups: employing more groups yields a higher computation time for solving the system of equations and more storage costs for the FMM data structures, while using less groups increases the assembly time and the memory requirements for the near BE part. The maximum and average truncation number are $p_{max} = 9$ and $p_{av} = 3$ for $R_{far} = 0.04$ and $\epsilon = 10^{-6}$.

Figure 5 presents a comparison between the measured levitation height vs time according to [8] and computed results for $\Delta t = 0.2$ ms and $\Delta t = 0.4$ ms obtained by means of the FMM accelerated hybrid FE-BE technique . A better agreement is observed as the time step diminishes. For a given time step, a finer mesh is not observed to improve significantly the accuracy.

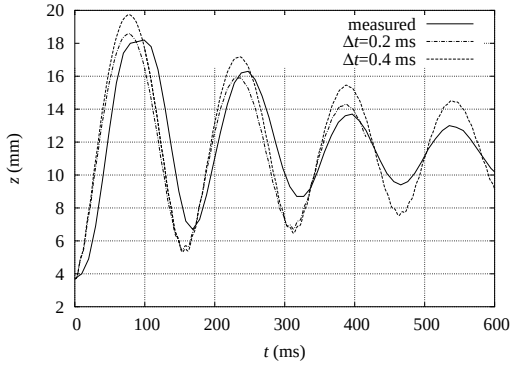

Fig. 5. Measured and calculated levitation height vs time

C. Computational cost

The system of algebraic equations is solved by means of the iterative solver GMRES [3] with ILU-preconditioning on a 400 MHz MIPS R12000 Processor.

The CPU time per time step and the memory requirements for the different discretisations (with Γ split up into 36, 45, 60, 60, 60, 77 and 77 groups, respectively) are shown in Table I. It illustrates the efficiency of the FMM as the number of BE unknowns increases. With the fourth mesh, e.g., the accelerated FE-BE analysis is roughly 16 times faster than the nonaccelerated one and the savings in memory approach 67%.

The grouping of the elements and the computation of the FMM data structures is done in a preprocessing that takes a few seconds, which is negligible in comparison to the total computational cost.

TABLE I
CPU TIME AND MEMORY REQUIREMENTS FOR DIFFERENT MESHES

Unknowns		FE-BE		FE-BE + FMM	
FE	BE	CPU (hours)	mem (Mb)	CPU (hours)	mem (Mb)
1473	520	0.41	21	0.15	18
2433	848	1.49	42	0.30	24
3633	1256	4.97	71	0.52	35
5073	1744	16.03	150	0.98	51
6753	2314	45.24	326	1.84	70
8673	2960	117.41	514	2.65	94
10833	3688	-	-	4.53	158

V. CONCLUSION

The resolution of a 3D eddy current problem by means of the FMM accelerated hybrid FE-BE model has been elaborated. An electrodynamic levitation device has been modelled taking into account the mechanical equation. An adaptive truncation scheme for the 3D Laplace Green function has been proposed.

A good agreement between the calculated results and the measurements has been observed. The efficiency of the FMM has been illustrated comparing the results obtained for different discretisations. Significant savings in computation time and storage requirements are achieved.

REFERENCES

[1] S. Kurz, J. Fetzer, G. Lehner and W. M. Rucker, "A novel formulation for 3D eddy current problems with moving bodies using a lagrangian description and BEM-FEM coupling," *IEEE Transactions on Magnetics*, vol. 34, no. 5, pp. 3068–3073, Sept. 1998.

[2] V. Rokhlin, "Rapid solution of integral equations of classical potential theory," *Journal of Computational Physics*, vol. 60, no. 2, pp. 187–207, 1985.

[3] Y. Saad and M. H. Schultz, "GMRES: A Generalized Minimal Residual Algorithm for solving nonsymmetric linear systems," *SIAM J. Sci. Comput.*, vol. 7, no. 3, pp. 856–869, July 1986.

[4] J. M. Song and W. C. Chew, "Multilevel fast-multipole algorithm for solving combined fi eld integral equations of electromagnetic scattering," *Micr. Opt. Tech. Lett.*, no. 1, pp. 14–19, Sept. 1995.

[5] K. Nabors and J. White, "FastCap: A multipole accelerated 3-D capacitance extraction program," *IEEE Transactions on Computer-Aided Design*, vol. 10, no. 11, pp. 1447–1459, November 1991.

[6] A. Buchau, C. J. Huber, W. Rieger and W. M. Rucker, "Fast BEM computations with the adaptive multilevel fast multipole method," *IEEE Transactions on Magnetics*, vol. 36, no. 4, pp. 680–684, July 2000.

[7] N. Lu and J.-M. Jin, "Application of fast multipole method to fi nite-element boundary-integral solution of scattering problems," *IEEE Transactions on Antennas and Propagation*, vol. 44, no. 6, pp. 781–786, June 1996.

[8] H. Karl, J. Fetzer, S. Kurz, G. Lehner and W. M. Rucker, "Description of TEAM workshop problem 28: An electrodynamic levitation device," `http://ics.ec.lyon.fr/team.html`.

[9] R. D. Graglia, 'On the numerical integration of the linear shape functions times the 3D Green's Function of its Gradient on a plane triangle," *IEEE Transactions on Antennas and Propagation*, vol. 41, no. 10, pp. 1448–1455, Oct. 1993.

[10] P. Dular, C. Geuzaine, W. Legros, "A natural method for coupling magnetodynamic h-formulation and circuit equations," *IEEE Transactions on Magnetics*, vol. 35, no. 3, pp. 1626–1629, May 1999.

[11] R. V. Sabariego, J. Gyselinck, C. Geuzaine, P. Dular and W. Legros, "Application of the fast multipole method to the 2D fi nite element-boundary element analysis of electromechanical devices," *COMPEL: The International Journal for Computation and Mathematics in Electrical and Electronic Engineering*, vol. 22, no. 3, pp. 659–673, 2003.